Carbohydrate Polymers 95 (2013) 262–271

Contents lists available at SciVerse ScienceDirect

Carbohydrate Polymers

journal homepage: www.elsevier.com/locate/carbpol

Fractionation and characterization of hemicelluloses from young bamboo (*Phyllostachys pubescens* Mazel) leaves

Hong Peng[a,b,*], Mengyang Zhou[a,b], Ziping Yu[a,b], Jinsheng Zhang[a,b], Roger Ruan[a,b,c,*], Yiqin Wan[a,b], Yuhuan Liu[a,b]

[a] Biomass Engineering Research Center, Ministry of Education, Nanchang University, Nanchang, Jiangxi 330047, PR China
[b] State Key Laboratory of Food Science and Technology, Nanchang University, Nanchang, Jiangxi 330047, PR China
[c] Center for Biorefining and Department of Bioproducts and Biosystems Engineering, University of Minnesota, St. Paul, MN 55108, USA

ARTICLE INFO

Article history:
Received 28 December 2012
Received in revised form 22 January 2013
Accepted 3 March 2013
Available online 13 March 2013

Keywords:
Bamboo leaves
Hemicellulosic polysaccharides
Chemical structure

ABSTRACT

Bamboo leaves are considered as an important source of bioactive molecules. In this work, leaves from young bamboo (*Phyllostachys pubescens* Mazel) aged 3 months were subjected to aqueous extraction and 2% NaOH solution extraction followed by precipitation in ethanol–water medium with different ethanol concentrations. The dissolved hemicellulosic polysaccharides presented a total recovery of 67.83% based on the total hemicellulose content in bamboo leaves. Chemical analysis of the fractions was performed by sugar composition analysis, Fourier-transform infrared spectrometry, and 1D nuclear magnetic resonance imaging. The results revealed that all polysaccharide fractions contained xylose, arabinose, glucose, galactose, ribose, and uronic acid. The polysaccharides from young bamboo leaves mainly consisted of arabinoxylans, arabinogalactans, and non-cellulosic β-D-glucans having (1→3)- and (1→4)-glucosidic linkages. The content of these polysaccharides was found to vary among the fractions depending on the separation method. Finally, the thermal behavior was also discussed.

1. Introduction

In the last decade, increasing attention has been paid to biorefinery processes for improving the utilization of lignocellulosic raw materials to obtain new sources of chemicals and energy that can replace oil-derived ones. Among the main components of lignocellulosic biomass, hemicellulosic polysaccharides are some of the most interesting biorefinery products. The term hemicellulose denotes a wide variety of polysaccharides isolated from plant cell wall.

As an important biomass, bamboo plants are commonly huge. Their stem, unlike those of other grasses, is distinctly wood-like and perennial, and their leaves survive more than one year. As the most economically valuable bamboo species, *Phyllostachys pubescens* Mazel is widely planted in China, with an annual production of about seven billion roots. Nowadays, large amounts of bamboo leaves are produced as a sub-product during the utilization process of bamboo. However, these bamboo leaves are unused and generally discarded, which is a waste of forestry resource and biomass because these leaves can be used to extract active polysaccharides (Wilkie & Woo, 1976, 1977) and generate high-value chemical compounds, such as flavonoids (Xie et al., 2013) and flavone-C-glycosides (Zhang, Jiao, Liu, Wu, & Zhang, 2008).

The chemical structure and physical property of hemicellulosic polysaccharides from bamboo stems have been extensively characterized (Luo, Peng, et al., 2012; Peng, Wang, et al., 2012; Peng, Zhang, et al., 2012; Peng, Peng, Bian, Xu, & Sun, 2011; Wen et al., 2011; Yang, Zhong, Yuan, Peng, & Sun, 2013). Wen et al. (2011) found that alkali-soluble hemicelluloses prepared from the bamboo *Bambusa rigida* consist a backbone of β-(1→4)-linked D-xylopyranosyl units with branches of arabinose and 4-*O*-methyl-D-glucuronic acid. The hemicelluloses fractionated by ionic liquid followed by alkaline extraction from the bamboo *Phyllostachys sulphurea (P. sulphurea)* were confirmed to consist mainly of 4-*O*-methyl-α-D-glucurono-α-L-arabino-β-D-xylans (Yang et al., 2013). In our previous research, arabinoxylans have been isolated from stems of the bamboo *P. pubescens* Mazel with different ages (Luo, Peng, et al., 2012; Peng, Wang, et al., 2012; Peng, Zhang, et al., 2012). The results demonstrate that the chemical properties of this bamboo's hemicelluloses slightly vary at different growing stages. Meanwhile, studies on bamboo leaf polysaccharides are limited (Wilkie & Woo, 1976, 1977). Wilkie and Woo (1976) found that the ratios of (1→3)- to (1→4)-glucosidic linkages in total hemicelluloses were as follows: 1:2.5 for leaves and 1:8.0 for stems of the bamboo *Arundinaria japonica (A. japonica)*; 1:2.6 for young and

* Corresponding authors at: Biomass Engineering Research Center, Ministry of Education, Nanchang University, Nanchang, Jiangxi 330047, PR China.
Tel.: +86 791 88333816; fax: +86 791 88333281.
E-mail addresses: penghpez@yahoo.com.cn (H. Peng), ruanx001@umn.edu (R. Ruan).

0144-8617/$ – see front matter © 2013 Elsevier Ltd. All rights reserved.
http://dx.doi.org/10.1016/j.carbpol.2013.03.007

1:2.4 for old leaves of the bamboo *Arundinaria anceps (A. anceps)*; and 1:19.5 for young and 1:15.6 for old nodes of the bamboo *A. anceps*. They also found that the structural properties of the hemicellulosic polysaccharides in bamboo leaves change with increased maturity (Wilkie & Woo, 1976), and that the composition and structural features of hemicellulosic polysaccharides in bamboo leaves generally differ from those in bamboo stems. However, the composition and structure of polysaccharides in leaves of the bamboo *P. pubescens* Mazel are far from being completely understood. Accordingly, our group was prompted to investigate the physicochemical characteristics of hemicellulosic polysaccharides in leaves of young *P. pubescens* Mazel bamboo. Given that physicochemical features are considered to be the basis of further utilization of hemicellulosic polysaccharides from young bamboo leaves, the chemical structure and thermal properties of young bamboo leaves must be elucidated.

In this study, water-soluble hemicellulosic polysaccharides and alkali-soluble fractions precipitated from ethanol–water media with different ethanol concentrations were isolated from delignified leaves of young *P. pubescens* Mazel bamboo aged 3 months. The composition and structural features of the various hemicelluloses were characterized by monosaccharide analysis, Fourier-transform infrared (FT-IR) spectrometry, and 1D nuclear magnetic resonance (1D NMR) imaging. The thermal properties were also evaluated by the thermogravimetry (TG)/differential thermogravimetry (DTG) technique. This research aimed to fractionate hemicellulosic polysaccharides, obtain structural information, and discuss thermal performance.

2. Materials and methods

2.1. Materials

The leaves of *P. pubescens* Mazel aged 3 months were collected at a local farm (Guanxi Village, Meiling Town, Nanchang City, China). The starting time of bamboo age was deemed as the point at which the bamboo shoots were above the ground. The young bamboo leaves were dried under sunlight and then ground to pass through a 40 mesh screen followed by a 100 mesh screen. The raw material was chemically characterized using standard methods of China (GB 2677.9-94, GB/T 2677.8-94, GB/T 2677.3-93, GB/T 2677.6-94, GB/T 2677.5-93, and GB/T 2677.5-93). The composition (%, w/w) of the young bamboo leaves was analyzed as cellulose 18.59%, hemicellulose 16.54%, Klason lignin 12.32%, ash 5.93%, benzene–ethanol extractives 10.27%, hot water extractives 18.99%, and 1% NaOH extractives 13.25% based on the weight of oven dried bamboo leaf powder. Distilled deionized water (Milli-Q) was used as the solvent for the preparation of all reagent solutions. Trimethylchlorosilane (TMS) (>99.9%) and hexamethyldisilane (HMDS) (>98.0%) were obtained from Sigma. All other reagents used were analytical grade.

2.2. Extraction of hemicellulosic polysaccharides from bamboo leaves

Hemicellulosic polysaccharides were extracted from bamboo leaves according to previous methods with slight modifications (Bian, Peng, Peng, Xu, & Sun, 2010; Peng et al., 2011). Fig. 1 shows the scheme for extracting hemicellulosic fractions with water and 2% NaOH. Briefly, wax-free bamboo leaf powder was delignified with 0.6% $NaClO_2$ at pH 4.2–4.7 for 2 h at 75 °C. Then, the delignified leaf holocellulose was extracted with distilled water at 80 °C for 3 h under a solid-to-liquid ratio of 1:20 (g/mL). After filtration, the filtrate was concentrated and then precipitated in three volumes of 95% ethanol, and the water-soluble hemicellulosic fraction was obtained after freeze drying. The water-insoluble residue was further treated with 2% NaOH at 55 °C for 2.5 h and filtered thereafter. The alkaline filtrate was neutralized with acetic acid to pH 5.5 and concentrated at reduced pressure. The concentrated solution containing alkali-soluble polysaccharides was precipitated in ethanol–water medium with different ethanol mass concentrations. Finally, four alkali-soluble hemicellulosic polysaccharide fractions were precipitated. Hereafter, BLH_W denotes the water-soluble hemicellulosic fraction extracted with distilled water at 80 °C for 3 h with a solid-to-liquid ratio of 1:20 (g/mL). BLH_{20}, BLH_{40}, BLH_{60}, and BLH_{80} denote the alkali-soluble hemicellulosic fractions isolated with 2% NaOH and sequentially precipitated in graded ethanol solutions with increased concentrations of 20%, 40%, 60%, and 80% ethanol, respectively.

2.3. Characterization of hemicelluloses

2.3.1. Sugar composition analysis

The total uronic acid content was analyzed by the *m*-hydroxybiphenyl method (Blumenkrantz & Asboe-Hansen, 1973). To determine the neutral sugar compositions of the five hemicellulosic fractions, 20 mg samples were hydrolyzed using 3.0 M trifluoro acetic acid (TFA) at 120 °C for 3 h in a 30 mL pressure vessel. The hydrolysate were then diluted with anhydrous ethanol, and the TFA was removed using a rotary vacuum evaporator at 45 °C. Anhydrous ethanol was added to the solids followed by re-evaporation. This procedure was repeated several times until the hydrolysates obtained were neutral. The dry hydrolysate solids were finally converted into their TMS derivatives and analyzed by gas chromatography–mass spectrometry (GC–MS) analyses (Peng, Sun, Zhang, and Lin, 2010). These analyses were performed on an Agilent 5973 GC-MS device equipped with a HP-5MS capillary column (30.0 m × 0.25 mm × 0.25 μm) and an ICIS data system. The carrier gas was He and the gas flow rate was 1.0 mL/min. Mass spectra were obtained by electron impact ionization at 70 eV. The oven temperature was programmed for 2 min at 60 °C, increased at 10 °C/min to 280 °C, and held for 5 min at 280 °C.

2.3.2. FT-IR spectrum analysis

For FT-IR measurements, the hemicellulose samples were blended with high-purity KBr to form pellets, and the spectra were obtained on a Nicolet 7500 FT-IR spectrophotometer (Thermo Nicolet Corporation, USA) between 4000 and 400 cm^{-1} at 4 cm^{-1} resolution.

2.3.3. NMR analysis

The solution-state ^1H NMR and ^{13}C NMR spectra were obtained at 30 °C on a Bruker MSL-600 MHz spectrometer (Bruker Corporation, Germany) with a 5 mm PABBO probe head. The ^1H NMR spectra were recorded at 600.5 MHz using 20 mg of hemicelluloses in 1.0 mL of DMSO-d_6 using TMS as an internal standard. The ^{13}C NMR spectra were recorded at 100.6 MHz and TMS was used as internal standard ($\delta = 0$ ppm) after 42,000 scans. Then, 80 mg samples were dissolved in 1.0 mL of DMSO-d_6 for ^{13}C NMR analysis.

2.3.4. Thermal analysis

Thermal analysis of the hemicelluloses was performed by TG/differential thermogravimetry (DTG) carried out on a TG/DTA PYRIS DIAMOND instrument (PE, USA). The measurements were recorded under nitrogen atmosphere at a flow rate of 50 mL/min and at a heating rate of 10 °C/min from room temperature to 700 °C. Approximately 1.9–5.7 mg of hemicelluloses was used. Calcined Al_2O_3 was used as a reference material in all experiments.

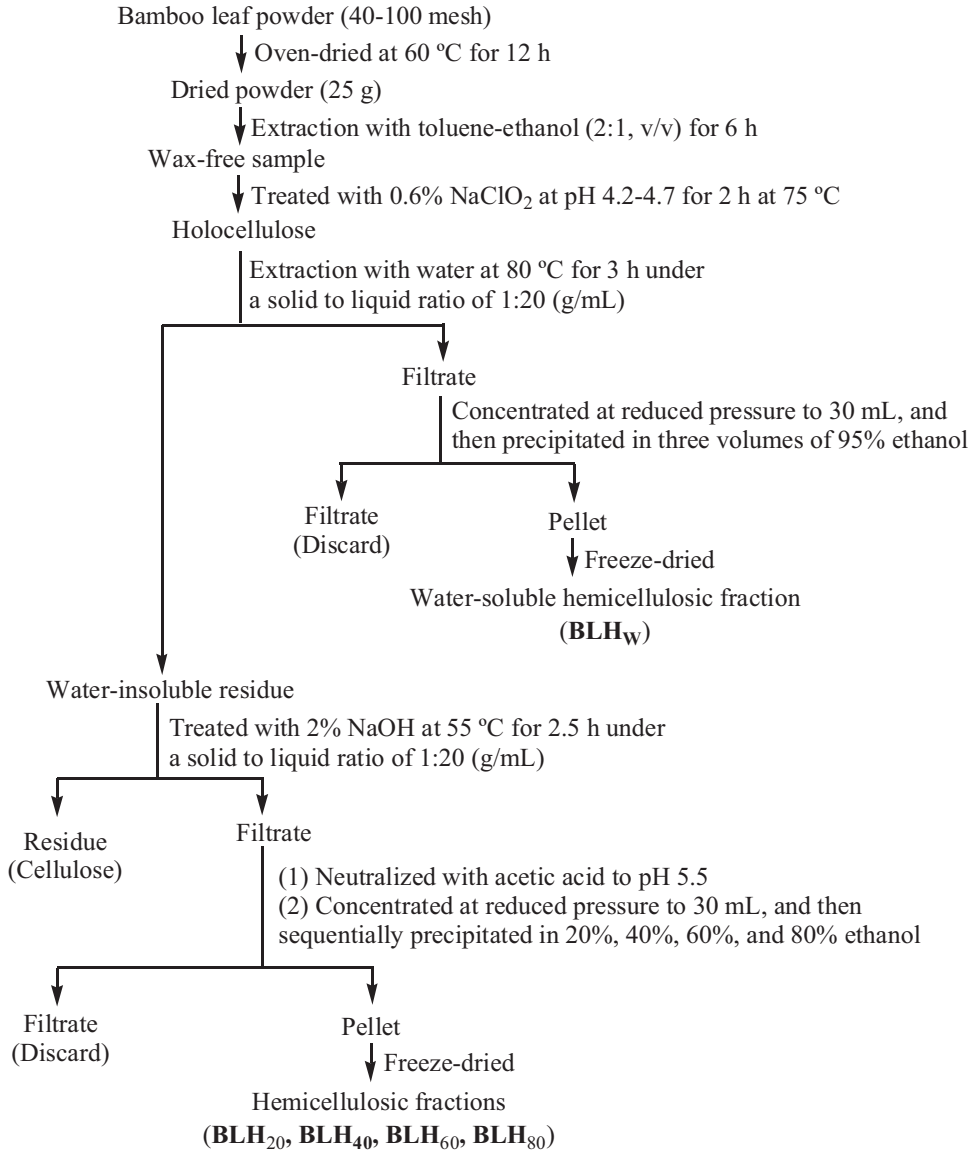

Fig. 1. Scheme of the extraction of hemicellulosic fractions from bamboo leaves.

3. Results and discussion

3.1. Yield of polysaccharide fractions

The yields of the five hemicellulosic fractions are shown in Table 1. Hot water removed 3.08% of the original hemicelluloses from bamboo leaf powder. In contrast to hot water, 2% NaOH extraction led to a much higher amount of hemicellulosic polysaccharides released. The alkali-soluble polysaccharides accounted for 64.75% based on the total hemicellulose content in bamboo leaves. At the same time, the yields significantly varied when ethanol solution with different mass concentrations was used to precipitate the polysaccharides. Precipitation with 60% ethanol resulted in the highest yield of hemicelluloses (27.69% based on the total hemicellulose content in bamboo leaves). Overall, 67.83% hemicelluloses were released during the entire separation process based on the total hemicellulose content in bamboo leaves. The total yield of the hemicellulosic fractions was nearly 11.22% based on the original weight of bamboo powder. The hemicellulose yield

Table 1
Yield of hemicellulosic polysaccharides isolated, and content of neutral sugars (relative percentage) and uronic acids (percentage dry sample, w/w) in the corresponding hemicellulosic fractions.

	Hemicellulosic fractions					Total
	BLH_W	BLH_{20}	BLH_{40}	BLH_{60}	BLH_{80}	
Yield[a] (%)	3.08	5.38	25.82	27.69	5.86	67.83
Yield[b] (%)	0.51	0.89	4.27	4.58	0.97	11.22
Arabinose	26.37	45.21	7.22	43.14	36.35	
Xylose	16.79	30.38	85.33	43.97	40.47	
Glucose	20.24	14.45	4.23	1.62	1.42	
Galactose	33.80	8.24	2.09	7.99	16.61	
Ribose	2.80	1.71	1.14	3.28	5.14	
Uronic acid	3.24	1.28	2.09	1.43	2.03	
Uro/Xyl	0.19	0.04	0.02	0.03	0.02	
Ara/Xyl	1.57	1.49	0.08	0.98	0.90	

[a] Based on the total hemicellulose content in bamboo leaves.
[b] Based on the original weight of dried bamboo leaf powder.

obtained by the method was not high, three factors should be considered. First, the wide range of particle size (40–80 mesh) of bamboo leaves may result in lower hemicellulose yield. Secondly, the alkali-soluble hemicelluloses extracted with 2% NaOH was only sequentially precipitated in ethanol–water medium with ethanol concentration of 20%, 40%, 60%, and 80%, respectively. Some hemicellulosic polysaccharides which could be precipitated out in ethanol–water medium with ethanol concentration higher than 80% have not been obtained. Finally, the water-insoluble residue was only treated with 2% NaOH at 55 °C for 2.5 h, many polysaccharides were still not been extracted. As a result, the total yield was only 67.83% based on the total hemicellulose content in bamboo leaves. Hemicellulosic polymers are a mixture of a number of different polysaccharides, and the yield of a polymer can generally vary depending on the separation method and extractant used in the experiment (Peng, Wang, et al., 2012; Wen et al., 2011).

3.2. Sugar composition analysis

Generally, the extraction and purification procedure used in this study afforded the variations in sugar composition and polysaccharide chemical structure. The neutral monosaccharide compositions and uronic acid content of the five hemicellulosic fractions are listed in Table 1. Monosaccharide analysis revealed that all fractions contained the same sugars. The dominance of xylose and a noticeable amount of arabinose in all fractions may identify them as arabinoxylans. In comparison with the alkali-soluble fractions, a significant difference was noticed in the water-soluble fraction BLH_W, in which a relatively higher content of glucose (20.24%) but a relatively lower quantity of xylose (16.79%) was observed. Thus, BLH_W may be composed of water-soluble non-cellulosic D-homoglucans having (1→3)- and (1→4)-glucosidic linkages (Wilkie & Woo, 1976). The water-soluble hemicelluloses BLH_W presented the highest glucose content (20.24%). Thus, it was qualitatively concluded that the water-soluble fraction contained the most water-soluble non-cellulosic heterolinked glucans. Glucose was also detected in the alkali-soluble fractions BLH_{20}, BLH_{40}, BLH_{60}, and BLH_{80}, demonstrating that water-insoluble glucans can be isolated from bamboo leaves by 2% NaOH at 55 °C for 2.5 h. Higher glucose was detected in the fraction precipitated in the solution with lower ethanol concentration, suggesting that more glucans were precipitated in ethanol–water medium having lower ethanol mass concentration. These results implied that the cell wall of young bamboo (*P. pubescens* Mazel) leaves contained non-cellulosic glucans, including water- and alkali-soluble glucans. The concomitant non-cellulosic glucans were impossible to separate completely from heteroxylans by graded precipitation with ethanol because of their strong bonding or structural association (Prozil, Costa, Evtuguin, Lopes, & Domingues, 2012). Obviously, arabinose (36.35–45.21%) and xylose (30.38–43.97%) were the major sugar components of the hemicellulosic fractions BLH_{20}, BLH_{60}, and BLH_{80} which underwent 20% NaOH extraction and graded ethanol precipitation. The highest amount of xylose was detected in the fraction BLH_{40} (85.33%) obtained by 40% ethanol precipitation, whereas the lowest was from the water-soluble fraction BLH_W (16.79%). The predominance of xylose in the fraction BLH_{40} suggested that the fraction BLH_{40} was rich in xylose and that it consisted of xylan polysaccharides. Galactose was found in the five preparations, pointing to the possible presence of residual arabinogalactans (Skendi, Biliaderis, Izydorczyk, Zervou, & Zoumpoulakis, 2011) and galactoarabinoxylans (Wilkie & Woo, 1976). A minor amount of ribose (1.14–5.14%) was also identified in all fractions, consistent with our earlier report wherein hemicelluloses from bamboo (*P. pubescens* Mazel) stems are found to contain a minor amount of ribose (Peng, Wang, et al., 2012). Finally, uronic acid (1.28–3.24%, mainly 4-*O*-methyl-α-D-glucuronic acid

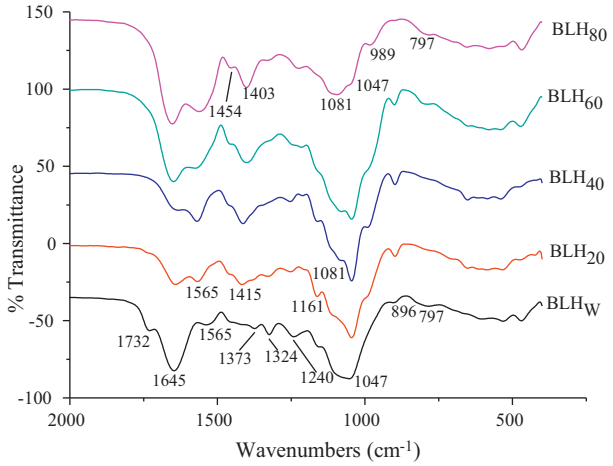

Fig. 2. FT-IR spectra of isolated polysaccharides.

together with minor amounts of galacturonic acid) was detected in all polysaccharides. The alkali-soluble fractions (BLH_{20}, BLH_{40}, BLH_{60}, and BLH_{80}) contained a relatively lower content of uronic acid than the water-soluble fraction (BLH_W). A possible reason was that uronic acid, as side chains in hemicellulosic polysaccharides, were partially cleaved or degraded in the alkaline solution. The ratio of uronic acid to xylose (Uro/Xyl) of hemicelluloses BLH_W extracted with hot water was much higher than those in the alkali-soluble fractions extracted with 2% NaOH. These results indicated that more acidic hemicelluloses were isolated with water. Variations in the arabinose to xylose (Ara/Xyl) ratio ranging from 0.08 to 1.57 were observed among the different fractions, implying some differences in their molecular structures. The Ara/Xyl ratios found in the water-soluble fraction BLH_W and the alkali-soluble fraction BLH_{20} precipitated in 20% ethanol were higher than those in the other three fractions precipitated in ethanol–water medium with higher ethanol concentrations.

3.3. FT-IR spectral analysis

FT-IR spectral analysis demonstrated that no significant difference was observed between water- and alkali-soluble fractions, except for minor differences in the intensity of bands. All samples gave the characteristic signals for O—H at about 3408 cm^{-1} and for C—H groups at about 2927 cm^{-1} (asymmetrical stretching) and 2873 cm^{-1} (symmetrical stretching) (not shown in Fig. 2) (Buranov and Mazza, 2012). The distinctive FT-IR absorptions of the polysaccharide samples appeared at 400–2000 cm^{-1} are given in Fig. 2. The FT-IR spectrum of fraction BLH_W showed a band at 1732 cm^{-1}, which originated from the carbonyl stretching vibration in acetyl ester groups of hemicelluloses (Buranov and Mazza, 2012; Sun et al., 2009). This band cannot be seen for the alkali-soluble fractions (BLH_{20}, BLH_{40}, BLH_{60}, and BLH_{80}), suggesting that the experimental conditions used significantly cleaved the ester bonds of the hemicelluloses by hydrolyzing the acetic acid esters, or that the amount of acetyl groups was too low. The absorption at 1646 cm^{-1} was attributed to absorbed water. The bands at 1565 and 1454 cm^{-1} originated from aromatic skeletal vibrations, indicating that the polysaccharides isolated were possibly contaminated with small amounts of lignin or ferulic acid residues esterified to the arabinoxylans (Skendi et al., 2011; Sun, Sun, Fowler, & Baird, 2005; Vazquez, Antorrena, Gonzalez, & Freire, 1997). The absorbance at 1403–1415, 1373, 1324, 1240, 1047, and 989 cm^{-1} were associated with hemicellulosic polysaccharides. Among them, the band at about 1403–1415 cm^{-1} represented the C—H bending vibration of —CH_2— (Kačuráková, Ebringerová, Hirsch, & Hromádková, 1994).

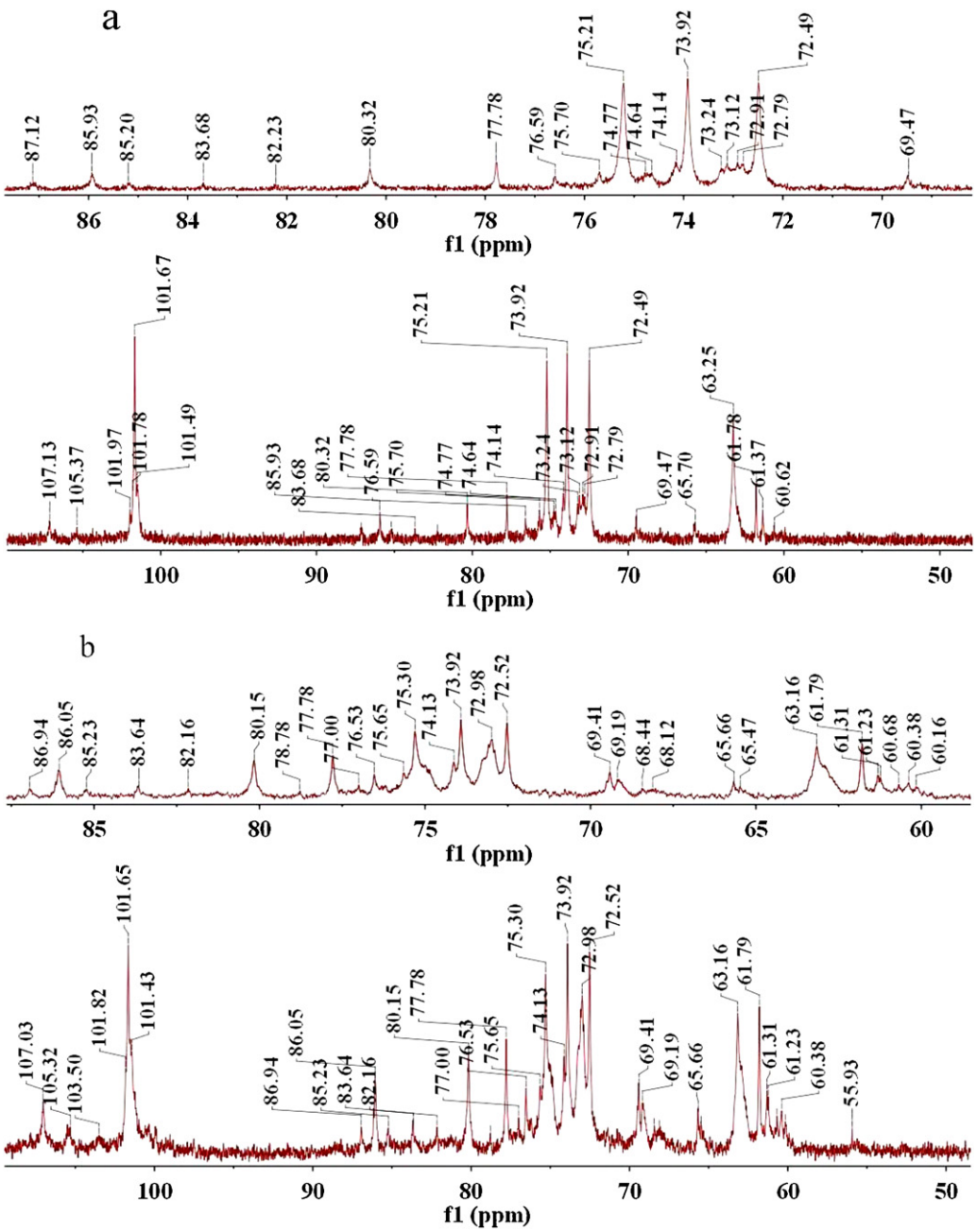

Fig. 3. ^{13}C NMR spectra of polysaccharide fractions BLH_{40} (a) and BLH_{60} (b) in DMSO-d_6 solvent.

The signal at 1373 cm^{-1} was attributed to —OH in-plane bending. The bands at 1324 and 1240 cm^{-1} indicated ring breathing with C—O stretching (Sandula, Kogan, Kacurakova, & Machova, 1999). Characteristically, the bands at 1081 and 1047 cm^{-1} suggested the presence of pyranose form of sugar in all the polysaccharides (Luo, Sun, Wu, & Yang, 2012; Tian et al., 2012; Zeng, Zhang, Gao, Jia, & Chen, 2012). The prominent absorption around 1047 cm^{-1} was assigned to the C—O, C—C stretching or C—OH bending vibration in linear and branched (1→4)-β-xylans such as glucuronoxylan and arabinoxylans (Kačuráková, Belton, Wilson, Hirsch, & Ebringerová, 1998; Kačuráková et al., 1994). The band shape was influenced by the galactan from the side chain, which had a band at 1081 cm^{-1} (Kačuráková, Capek, Sasinková, Wellner, & Ebringerová, 2000). The galactosyl units were linked together by β-(1→6) or β-(1→3) linkage. At the same time, the band at 1081 cm^{-1} was undetected in the FT-IR spectra of the fractions BLH_W and BLH_{20}, suggesting that the water-soluble fraction and fraction precipitated in 20% ethanol did not contain the galactan from the side chains. The presence of arabinosyl side chains was indicated by low-intensity shoulders at 1161 and 989 cm^{-1} (Kačuráková et al., 1998). The small shoulder peak at 1161 cm^{-1} in all spectra corresponded to the glycosidic bond vibrations (C—O—C) of arabinosyl side chain in the anometric region (Xiao, Sun, & Sun, 2001). The absence of the peak at 1162 cm^{-1} for the fractions BLH_{60} and BLH_{80} implied that the arabinosyl units of side chain were not in the anometric region. The low intensity of the band at 989 cm^{-1} indicated the presence of arabinose attached at the position O-3 of the xylopyransyl constituents (Ebringerová, Hromádková, Alföldi, & Berth, 1992). The band at 989 cm^{-1} for the water-soluble fraction BLH_W was undetected, suggesting that no arabinosyl side chains attached at the position *O*-3 of the xylopyransyl constituents. The absence of the peaks at 1026 and 920 cm^{-1} indicated that α-glucans such as starch did not exist in the five

Table 2
Assignment of signals in the ^{13}C NMR and ^{1}H NMR spectra of the fractions.

δ_C (ppm)	δ_H (ppm)	Assignment	Structural units
175.20		C-6	4-*O*-Methyl-α-D-glucuronic acid
107.13		C-1	α-L-Arabinofuranosyl
103.57		C-1	β-D-Xylopyranosyl
101.78		C-1	(1→4)-Linked-β-D-xylopyranosyl at non-reducing end
101.67	4.27	C-1/H-1	3-*O*-Acetyl-(1→4)-linked-β-D-xylopyranosyl
101.49	4.95	C-1/H-1	β-D-Glucopyranosyl
99.95		C-1	α-L-Galactopyranosyl
85.93	3.97	C-4/H-4	α-L-Arabinofuranosyl
82.23		C-4	4-*O*-Methyl-α-D-glucuronic acid
80.33	3.82	C-2/H-2	α-L-Arabinofuranosyl
78.78		C-4	β-D-Glucopyranosyl
77.78	3.69	C-3/H-3	α-L-Arabinofuranosyl
77.00		C-4	Internal (1→4)-linked-β-D-xylopyranosyl
76.59		C-5	4-*O*-Methyl-α-D-glucuronic acid
75.21	3.63	C-4/H-4	(1→4)-Linked-β-D-xylopyranosyl
74.77	4.76	C-3/H-3	3-*O*-Acetyl-(1→4)-linked-β-D-xylopyranosyl
74.14		C-3	β-D-Glucopyranosyl
73.92	3.26	C-3/H-3	(1→4)-Linked-β-D-xylopyranosyl
73.24	4.49	C-2/H-2	2-*O*-Acetyl-(1→4)-linked-β-D-xylopyranosyl
73.12		C-3	4-*O*-Methyl-α-D-glucuronic acid
72.91		C-2	4-*O*-Methyl-α-D-glucuronic acid
72.49	3.05	C-2/H-2	(1→4)-Linked-β-D-xylopyranosyl
69.47		C-4	(1→4)-Linked-β-D-xylopyranosyl at non-reducing end
69.19		C-3	α-L-Galactopyranosyl
65.70		C-5	(1→4)-Linked-β-D-xylopyranosyl at non-reducing end
63.25	3.87/3.16	C-5/H-5_{eq} [a]/H-5_{ax} [b]	(1→4)-Linked-β-D-xylopyranosyl
61.78	3.46	C-5/H-5	α-L-Arabinofuranosyl
61.37		C_α-6	α-L-Galactopyranosyl
61.23		C_β-6	α-L-Galactopyranosyl
60.62		C-6	β-D-Glucopyranosyl
	5.45	H-1	α-L-Arabinofuranosyl linked to *O*-3 of xylan
	5.33	H-1	α-L-Arabinofuranosyl linked to *O*-2 of xylan
	4.99	H-1	4-*O*-Methyl-α-D-glucuronic acid
	3.51	H-2	β-D-Glucopyranosyl
	3.36	OCH_3	4-*O*-Methyl-α-D-glucuronic acid
	2.55	$-CH_2-$	Residual ethanol
	2.51	$-CD_3$	DMSO-d_6
	1.67	$-CH_3$	Residual ethanol

[a] The equatorial proton linked at C-5 of (1→4)-linked-β-D-xylopyranosyl.
[b] The axial proton linked at C-5 of (1→4)-linked-β-D-xylopyranosyl.

isolated polysaccharides (Kačuráková et al., 2000; Ying, Han, & Li, 2011). A weak band at 896 cm^{-1} corresponded to the C-1 group frequency or ring frequency, which was characteristic of β-glycosidic linkages between the sugar units (Gupta, Madan, & Bansal, 1987). The symmetrical stretching vibration of C—O—C of glucopyranose was observed at about 797 cm^{-1}. Considering the low uronic acid content, the peaks at 1100 and 1018 cm^{-1} diminished (Coimbra, Barros, Barros, Rutledge, & Delgadillo, 1998).

3.4. NMR analysis

To elucidate further the structural features of the hemicellulosic polysaccharides, the fractions BLH_{40} and BLH_{60} were selected to be investigated using ^{1}H NMR and ^{13}C NMR techniques. NMR signals were assigned by comparison with published literature (Allerdings, Ralph, Steinhart, & Bunzel, 2006; Bian et al., 2010; Kardošová et al., 2001; Kim et al., 2011; Li, Fan, Xu, & Sun, 2011; Lisboa, Evtuguin, Neto, & Goodfellow, 2005; Peng, Zhang, et al., 2012; Sun, Jing, Fowler, Wu, & Rajaratnam, 2011; Sun et al., 2005; Yang et al., 2013; Yuan, Sun, Xu, & Sun, 2011;).

The ^{13}C NMR spectrum of the hemicellulosic polysaccharide BLH_{40} is displayed in Fig. 3a. The assignments of the fractions are listed in Table 2. The absence of peaks in the region 110–160 ppm indicated low concentration of residual lignin (Yang et al., 2013). The anomeric carbon signal of (1→4)-linked-β-D-xylopyranosyl units acetylated at C-3 was found at 101.67 ppm (Peng, Zhang, et al., 2012; Yuan et al., 2011). In the aliphatic regions, the C-2 signal from 2-*O*-acetyl-β-D-xylopyranosyl units and the C-3 signal from 3-*O*-acetyl-β-D-xylopyranosyl units were observed at 73.24 and 74.77 ppm, respectively (Yuan et al., 2011). The observation of ^{13}C NMR signals from *O*-acetyl substituted xylopyranosyl units indicated that extraction with 2% NaOH cannot completely break this ester bond. Other signals from β-D-xylopyranosyl residues were evidently noted with its signals at 72.49 (C-2), 73.92 (C-3), and 75.21 (C-4) ppm, respectively, but the feature of C-5 was at 63.25 ppm (Bian et al., 2010; Peng, Zhang, et al., 2012; Sun, Jing, et al., 2011; Sun et al., 2005; Yuan et al., 2011). The existence of β-D-xylopyranosyl residues at non-reducing end was confirmed by the observation of three signals at 101.78 (C-1), 69.47 (C-4), and 65.70 (C-5) ppm (Kardošová et al., 2001). In ^{13}C NMR spectra, the signals at 107.13 (C-1), 85.93 (C-4), 80.33 (C-2), 77.78 (C-3), and 61.78 (C-5) ppm were characteristic of α-L-arabinofuranosyl units (Peng, Zhang, et al., 2012; Sun et al., 2005; Yang et al., 2013). The signals observed at 82.23 (C-4), 76.59 (C-5), 73.12 (C-3), and 72.91 (C-2) ppm were characteristic of 4-*O*-methyl-α-D-glucuronic acid (Yang et al., 2013; Yuan et al., 2011). Among other signals in ^{13}C NMR spectra, the signal of —COOH at C-6 of 4-*O*-methyl-α-D-glucuronic acid residues was observed at 175.20 ppm (value not shown in Fig. 3a). The anomeric signals from β-D-glucopyranosyl units were clearly found at 101.49 ppm, whereas the signals at 74.14 and 60.62 ppm corresponded to C-3 and C-6 (Li et al., 2011; Yang et al., 2013). This result confirmed the presence of non-cellulosic β-D-glucans. The Cα-6 signal of α-L-galactopyranosyl units was observed at 61.37 ppm. The resonances at 105.37, 101.97, 87.12, 85.20, 83.68, 74.64, and 72.79 ppm were unassigned.

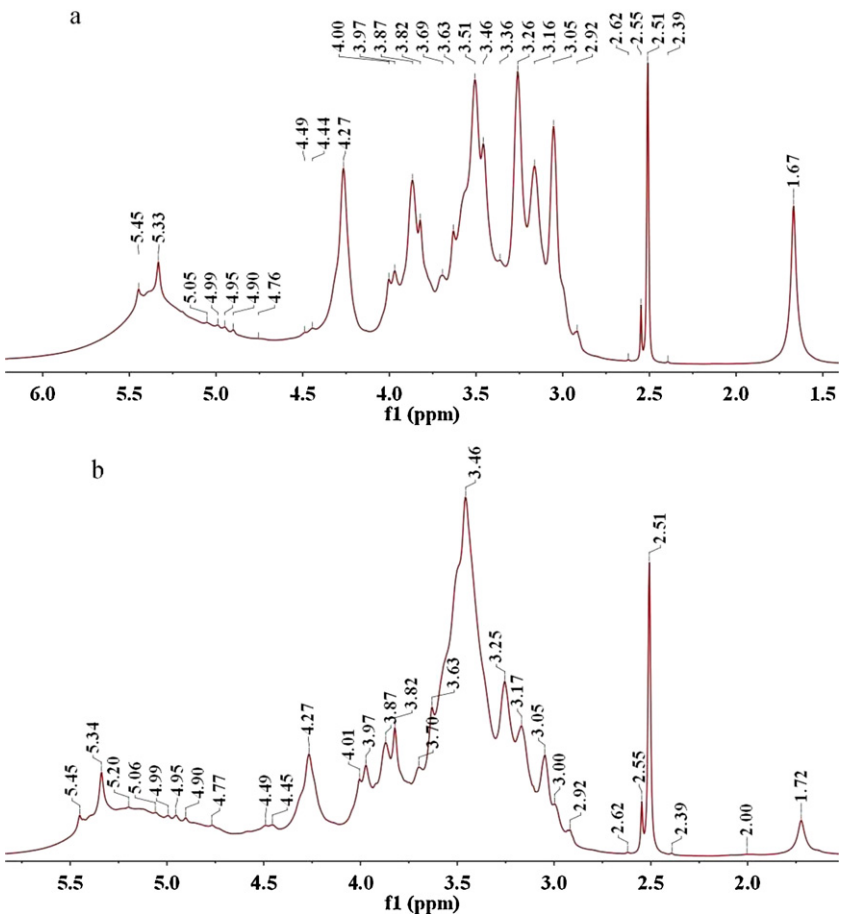

Fig. 4. ^{1}H NMR spectra of the polysaccharide fraction BLH_{40} (a) and hemicellulosic fraction BLH_{60} (b) in DMSO-d_6 solvent.

The ^{13}C NMR spectrum of the hemicellulosic polysaccharide BLH_{60} is shown in Fig. 3b. The spectrum was similar with that of the fraction BLH_{40} (Fig. 3a), except for minor differences in the chemical shift and signal intensity to a certain degree, which suggested that the fraction BLH_{60} had a similar backbone to the fraction BLH_{40}. However, a few new peaks appeared in the ^{13}C NMR spectrum of the hemicellulosic polysaccharides BLH_{60}, and the assignments are also listed in Table 2. In Fig. 3b the corresponding anomeric signal of β-D-xylopyranosyl units at 103.50 was observed (Yuan et al., 2011). The presence of the signals at 99.95, 69.19, and 61.31 (α) and 61.23 (β) ppm were accordant with the chemical shifts of C-1, C-3, and C-6 in α-L-galactopyranosyl units with α and β conformations (Allerdings et al., 2006). Compared with the ^{13}C NMR spectrum of BLH_{60} (Fig. 3b), the signals corresponding to the chemical shifts of C-1, C-3, and $C_β$-6 in α-L-galactopyranosyl units in BLH_{40} were absent. This phenomenon was related to the low content of galactose in BLH_{40} than that in BLH_{60} (Table 1). The signal at 78.78 ppm was attributed to C-4 of β-D-glucopyranosyl units. The weak signal of C-4 from unsubstitued internal β-D-xylopyranosyl residues was detected at 77.00 ppm (Sun et al., 2005). An important signal at 55.93 ppm characteristic of methoxyl from lignin was observed (Kim et al., 2011). However, this signal was absent in BLH_{40}. The coexisting signals at 86.94, 86.05, 80.15, 68.44, 68.12, 65.47, 60.38, and 60.16 ppm were undetermined.

The ^{1}H NMR spectra of BLH_{40} and BLH_{60} are shown in Fig. 4, and the main assignments of the fractions are listed in Table 2. The similar ^{1}H NMR spectra of BLH_{40} and BLH_{60} further implied that the core structure of the hemicellulosic polysaccharides precipitated in 40% and 60% ethanol insignificantly differed. However, the intensities obviously varied between the hemicellulosic fractions BLH_{40} and BLH_{60}. The α-anomeric signals, β-anomeric signals, and ring proton signals occurred in the regions between 5.5 and 4.9, 4.9

Table 3
Thermogravimetric characteristics.

Sample	Temperature range (°C)	T_{peak} (°C)	Weight loss (%)	Maximum weight loss rate (%/min)	Residue at 700 °C (%)	Total weight loss (%)
BLH_W	199–383	286	48.78	4.00	25.03	74.97
	483–516	493	2.29	1.07		
	557–637	615	3.48	0.72		
BLH_{20}	197–354	297	60.71	8.14	19.83	80.17
BLH_{40}	194–359	288	54.60	7.66	25.45	74.55
BLH_{60}	199–370	286	43.98	4.56	31.81	68.19
	510–555	534	2.14	0.70		
BLH_{80}	200–380	298	34.39	3.07	35.33	64.67
	501–544	527	3.64	1.32		

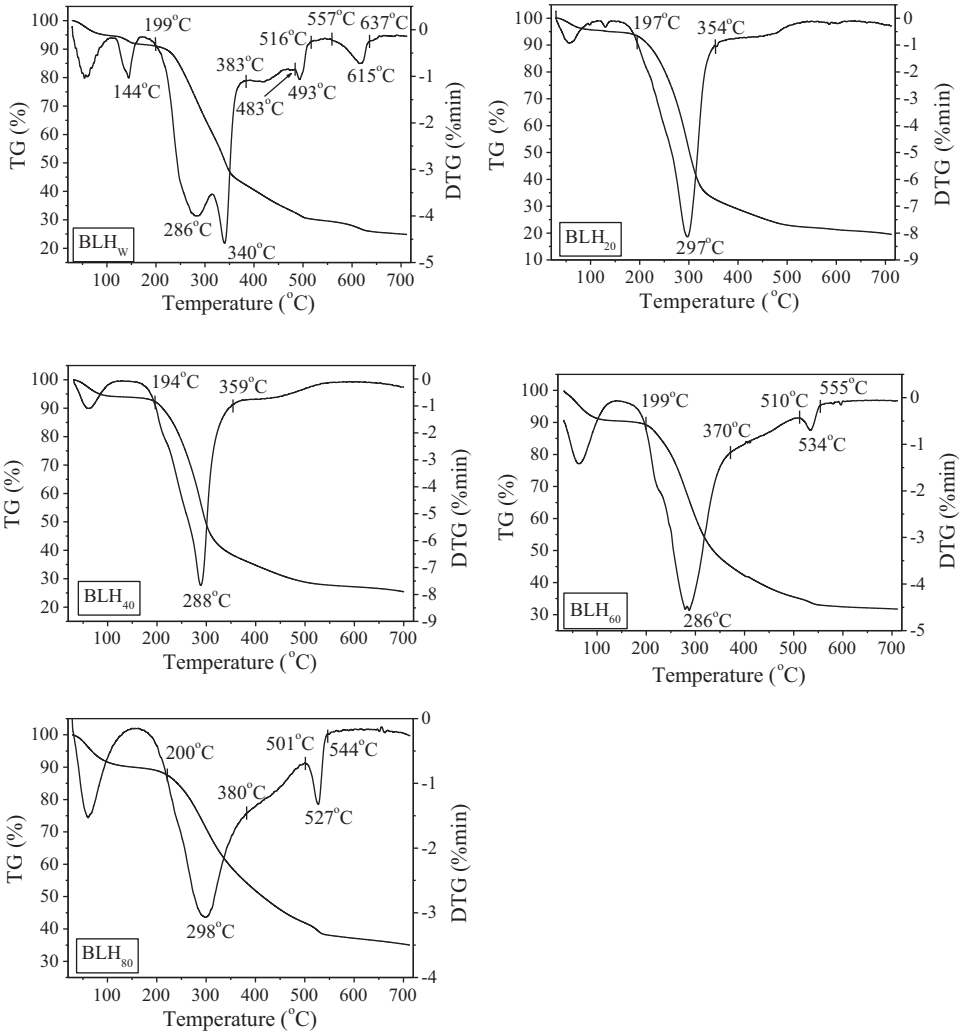

Fig. 5. TG-DTG curves of the polysaccharide fractions.

and 4.0, and 4.0 and 3.0 ppm, respectively. The anomeric protons of terminal arabinofuranosyl units linked to *O*-3 and *O*-2 of xylans were indicated by two weak resonances at 5.45 and 5.33 (5.34 in Fig. 4b) ppm (Sun et al., 2005). The weak signals at 4.99 (H-1) and 3.36 (OCH_3) ppm were attributed to 4-*O*-methyl-α-D-glucuronic acid residues (Bian et al., 2010). In Fig. 4b, the signal at 3.36 ppm was overlapped by other signals. The β-anomeric proton signal of (1→4)-linked-β-D-xylopyranosyl units acetylated at C-3 was observed at 4.27 ppm (Peng, Zhang, et al., 2012; Yuan et al., 2011), and the β-anomeric proton signal at 4.20 ppm corresponding to β-D-xylopyranosyl units was not found (Yuan et al., 2011). The signals at 4.49 and 4.76 ppm in ^{1}H NMR spectra of BLH_{40} and BLH_{60} were assigned to H-2 from 2-*O*-acetyl-β-D-xylopyranosyl units and H-3 from 3-*O*-acetyl-β-D-xylopyranosyl units, respectively (Yuan et al., 2011). The absence of the signal at 2.0 ppm, originating from aliphatic acetates (acetyl groups in hemicelluloses) in both the BLH_{40} and BLH_{60} spectra, was good evidence of ester bond cleavage during hemicellulosic polysaccharide extraction with 2% NaOH (Kim et al., 2011). The signals corresponding to H-2, H-3, H-4, and H-5 of β-D-xylopyranosyl units appeared at 3.05, 3.26 (3.25 in Fig. 4b), 3.63, and 3.87/3.16 (3.17 in Fig. 4b) ppm, respectively (Bian et al., 2010; Peng, Zhang, et al., 2012; Sun, Jing, et al., 2011; Sun et al., 2005; Yuan et al., 2011). The chemical shifts of 3.87 and 3.16 (3.17 in Fig. 4b) ppm originated from the equatorial and axial protons linked at C-5 of β-D-xylopyranosyl units, respectively, whereas the signals at 3.97, 3.82, 3.69 (3.70 in Fig. 4b), and 3.46 ppm were assigned to H-4, H-2, H-3, and H-5, respectively, in the α-L-arabinofuranosyl units (Peng, Zhang, et al., 2012). A strong signal for β-D-glucopyranosyl units in BLH_{40} was observed at 3.51 (H-2) ppm (Fig. 4a) (Li et al., 2011; Lisboa et al., 2005), whereas this peak of β-D-glucopyranosyl units in BLH_{60} was overlapped (Fig. 4b). Furthermore, β-D-glucopyranosyl units gave very weak signal at 4.95 ppm for β-anomeric protons in the ^{1}H NMR spectra. The two resonances observed at 2.55 and 1.67 (1.72 in Fig. 4b) ppm represented the methylene and methyl groups in the residual ethanol (Bian et al., 2010). The strong signal at 2.51 ppm was attributed to DMSO-d_6 solvent. The minor peaks at 5.05, 4.90, 4.44, 4.00, 2.92, 2.62, and 2.39 ppm in Fig. 4a, as well as the peaks at 5.20, 5.06, 4.45, 4.01, 3.00, 2.92, 2.62, 2.39, and 2.00 ppm in Fig. 4b were unassigned.

As shown in Figs. 3 and 4, the spectra of hemicellulosic polysaccharides BLH_{40} and BLH_{60} were similar. Both spectra showed prominent signals corresponding to β-D-xylopyranosyl units, α-L-arabinofuranosyl units, 4-*O*-methyl-α-D-glucuronic acid, β-D-glucopyranosyl units, and α-L-galactopyranosyl units. Based on the sugar composition, FT-IR, and NMR spectral analysis, the hemicellulosic polysaccharides isolated from young bamboo (*P. pubescens* Mazel) leaves can be structurally defined as 4-*O*-methyl-α-glucurono-arabinoxylans, arabinogalactans, and non-cellulosic β-D-glucans having (1→3)- and (1→4)-glucosidic linkages. The

contents of these structural elements varied based on the isolation and precipitation method.

3.5. Thermal property

The TG-DTG curves of the five polysaccharide fractions at a heating rate of 10 °C/min are shown in Fig. 5, and the results are listed in Table 3. Obviously, the low temperature stage (below 194 °C) was ascribed to the loss of moisture and volatile ingredients. The fast thermal decomposition occurred within 194–384 °C. At this stage, significant loss of sample mass occurred, varying from 34.39% to 60.71% of the original weight (Table 3). All fractions began to decompose at significant rates when the temperature was higher than 194 °C, and the initial degradation temperatures were similar. The peak temperatures at maximum rate of weight loss occurred at 286, 297, 288, 286, and 298 °C for BLH_W, BLH_{20}, BLH_{40}, BLH_{60}, and BLH_{80}, respectively (Fig. 5). All peak temperatures were within a narrow range of 286–298 °C. The corresponding maximum weight loss rates were 4.00%, 8.14%, 7.66%, 4.56%, and 3.07% per minute (Table 3). In the rapid weight loss stage, the mass loss of fraction BLH_{20} precipitated in 20% ethanol was the highest (60.71%), and the fraction BLH_{80} precipitated in 80% ethanol had the lowest mass loss of 34.39%. In addition, for the four alkali-soluble fractions which were precipitated out by ethanol–water medium with different ethanol concentration, the weight loss decreased with the increase of ethanol concentration. It was to say that during the fast pyrolysis period the thermal stability increased with the increase of ethanol concentration. The differences between the weight loss and maximum rate of weight loss in the main degradation stage were possibly due to the structural inhomogeneity of the fractions and mutual differences in the relative content of the constituents (Sun, Wen, Xu, & Sun, 2011). The sharp shoulder peak in the DTG curve of BLH_W was observed at 340 °C in the major degradation zone (Fig. 5). This rapid mass loss possibly originated from the rapid thermal pyrolysis of the water-soluble non-cellulosic heterolinked glucans with (1→3)- and (1→4)-glucosidic linkages. There were no shoulder peaks observed in the DTG curve of the four alkali-soluble fractions. One possible reason was that the alkali-soluble fractions contained less glucans compared to the water-soluble one. Based on the TG-DTG curves of BLH_W, BLH_{60}, and BLH_{80}, some small weight loss steps were observed from 483 °C to 637 °C. For the water-soluble polysaccharide fraction BLH_W, two small weight loss steps were found: one with a weight loss of 2.29% between 483 and 516 °C, and another one with a weight loss of 3.48% between 557 and 637 °C. Temperature peaks with weaker intensity were discovered at 493 and 615 °C respectively, and the corresponding maximum pyrolysis rates were 1.07% and 0.72% per minute. At the same time, the polysaccharides BLH_{60} and BLH_{80} showed a small weight loss step between 510 and 555 °C, as well as between 501 and 544 °C, respectively. Decomposition ranging from 483 to 637 °C was suggested to proceed through the degradation of the volatile components, forming char (Sun, Wen, et al., 2011; Yang, Yan, Chen, Hee, & Zheng, 2007; Yang et al., 2006). Coincidentally, the thermal behavior of fraction BLH_{20} was similar to that of fraction BLH_{40}. The fraction BLH_{60} also presented the similar thermal behavior as the fraction BLH_{80}, and the main weight loss step was followed by a low, flat TG signal, which may be due to a slow step-by-step decomposition (charring) of the residue. As a result, at the final temperature of 700 °C, the total weight losses of the original mass were 74.97% for BLH_W, 80.17% for BLH_{20}, 74.55% for BLH_{40}, 68.19% for BLH_{60}, and 64.67% for BLH_{80} (Table 3). Most of the samples decomposed under N_2 atmosphere from room temperature to 700 °C at a heating rate of 10 °C/min. During the whole decomposition process, the total weight loss of the fraction BLH_{80} was the lowest, and the one of the fraction BLH_{20} was the highest. The total weight loss of water-soluble hemicelluloses BLH_W was similar with that of the alkali-soluble fraction BLH_{40} which was precipitated out in 40% ethanol solution. On the other hand, the polysaccharide fraction BLH_{20} precipitated in 20% ethanol exhibited the lowest thermal stability, whereas the fraction BLH_{80} precipitated in 80% ethanol showed the strongest thermal stability. The water-soluble fraction presented similar stability with the fraction BLH_{40}. For the four alkali-soluble fractions precipitated out by ethanol–water medium with different ethanol concentration, the thermal stability increased with the increase of ethanol concentration. Their structures probably contributed to the variations in thermal stability.

4. Conclusions

Water-soluble hemicellulosic polysaccharides (BLH_W) and alkali-soluble polysaccharides were isolated from the leaves of young *P. pubescens* Mazel bamboo aged 3 months using hot water and 2% NaOH as extractant. The alkali-soluble polysaccharides were precipitated in graded ethanol solutions with increased mass concentrations of 20%, 40%, 60%, and 80% ethanol, respectively, resulting in the corresponding fractions of BLH_{20}, BLH_{40}, BLH_{60}, and BLH_{80}. The yields significantly varied with the ethanol concentration. Hot water and 2% NaOH totally removed 67.83% hemicellulosic polysaccharides from *P. pubescens* Mazel leaves. All polysaccharides contained arabinose, xylose, glucose, galactose, ribose, and uronic acid. For alkali-soluble polysaccharides, with increased ethanol mass concentration, the obtained fractions contained lower glucose content. In addition to 4-*O*-methyl-α-glucurono-arabinoxylans, both arabinogalactans and non-cellulosic β-D-glucans having (1→3)- and (1→4)-glucosidic linkages were found in all fractions isolated from young *P. pubescens* Mazel leaves. The contents of these structural elements in each fraction were related to the separation and precipitation methods. More acidic hemicelluloses were isolated using hot water as extractant. For all polysaccharide fractions, a significant loss of sample mass occurred from 194 °C to 384 °C, with weight losses varying from 34.39% to 60.71%. At the final temperature of 700 °C, the total weight losses were between 64.67% and 80.17%. Most samples decomposed under N_2 atmosphere from room temperature to 700 °C at a heating rate of 10 °C/min. The water-soluble fraction exhibited similar thermal stability with the alkali-soluble fraction precipitated out in 40% ethanol. For the alkali-soluble fractions, the thermal stability increased with the increase of ethanol concentration of precipitation solution. These results helped elucidate the chemical structure and thermal behavior of hemicellulosic polysaccharides from young *P. pubescens* Mazel leaves.

Acknowledgements

The authors are grateful for financial support of the Natural Science Foundation of China (30960304 and 21266022), of the National High Technology Research and Development Programme of China (863 Program) (2012AA021205-6), and of the Research Programme of Sate Key Laboratory of Food Science and Technology, Nanchang University (SKLF-TS-201111).

References

Allerdings, E., Ralph, J., Steinhart, H., & Bunzel, M. (2006). Isolation and structural identification of complex feruloylated heteroxylan side-chains from maize bran. *Phytochemistry*, *67*(12), 1276–1286.

Bian, J., Peng, F., Peng, P., Xu, F., & Sun, R. C. (2010). Isolation and fractionation of hemicelluloses by graded ethanol precipitation from *Caragana korshinskii*. *Carbohydrate Research*, *345*(6), 802–809.

Blumenkrantz, N., & Asboe-Hansen, G. (1973). New method for quantitative determination of uronic acid. *Analytical Biochemistry*, *54*(2), 484–489.

Buranov, A. U., & Mazza, G. (2012). Fractionation of flax shives with pressurized aqueous ethanol. *Industrial Crops and Products*, *35*(1), 77–87.

Coimbra, M. A., Barros, A., Barros, M., Rutledge, D. N., & Delgadillo, I. (1998). Multivariate analysis of uronic acid and neutral sugars in whole pectic samples by FT-IR spectroscopy. *Carbohydrate Polymers*, *37*(3), 241–248.

Ebringerová, A., Hromádková, Z., Alföldi, J., & Berth, G. (1992). Structure and solution properties of corn cob heteroxylans. *Carbohydrate Polymers*, *19*(2), 99–105.

Gupta, S., Madan, R. N., & Bansal, M. C. (1987). Chemical composition of *Pinus caribaea* hemicellulose. *Tappi Journal*, *70*(8), 113–114.

Kačuráková, M., Belton, P. S., Wilson, R. H., Hirsch, J., & Ebringerová, A. (1998). Hydration properties of xylan-type structures: In FT-IR study of xylooligosaccharides. *Journal of the Science of Food and Agriculture*, *77*(1), 38–44.

Kačuráková, M., Capek, P., Sasinková, V., Wellner, N., & Ebringerová, A. (2000). FT-IR study of plant cell wall model compounds: Pectic polysaccharides and hemicelluloses. *Carbohydrate Polymers*, *43*(2), 195–203.

Kačuráková, M., Ebringerová, A., Hirsch, J., & Hromádková, Z. (1994). Infrared study of arabinoxylans. *Journal of the Science of Food and Agriculture*, *66*(3), 423–427.

Kardošová, A., Ebringerová, A., Alföldi, J., Nosálóvá, G., Mátáková, T., & Hříbalová, V. (2001). Structural features and biological activity of an acidic polysaccharide complex from *Mahonia aquifolium* (Pursh) Nutt. *Carbohydrate Polymers*, *57*(2), 165–176.

Kim, J.-Y., Shin, E.-J., Eom, I.-Y., Won, K., Kim, Y. H., Choi, D., et al. (2011). Structural features of lignin macromolecules extracted with ionic liquid from poplar wood. *Bioresource Technology*, *102*(19), 9020–9025.

Li, M. F., Fan, Y. M., Xu, F., & Sun, R. C. (2011). Structure and thermal stability of polysaccharide fractions extracted from the ultrasonic irradiated and cold alkali pretreated bamboo. *Journal of Applied Polymer Science*, *121*(1), 176–185.

Lisboa, S. A., Evtuguin, D. V., Neto, C. P., & Goodfellow, B. J. (2005). Isolation and structural characterization of polysaccharides dissolved in Eucalyptus globules kraft black liquors. *Carbohydrate Polymers*, *60*(1), 77–85.

Luo, Q., Peng, H., Zhou, M. Y., Lin, D., Ruan, R., Wan, Y. Q., et al. (2012). Alkali extraction and physicochemical characterization of hemicelluloses from young bamboo (*Phyllostachys pubescens* Mazel). *Bioresources*, *7*(4), 5817–5828.

Luo, Q., Sun, Q., Wu, L. S., & Yang, Z. R. (2012). Structural characterization of an immunoregulatory polysaccharide from the fruiting bodies of *Lepista sordida*. *Carbohydrate Polymers*, *88*(3), 820–824.

Peng, H., Sun, Y., Zhang, J. H., & Lin, L. (2010). Degradation of cellooligosaccharides in oxidative medium and alkaline medium: HPLC, FTIR, and GC–MS analysis. *Bioresources*, *5*(2), 616–633.

Peng, H., Wang, N., Hu, Z. R., Yu, Z. P., Liu, Y. H., Zhang, J. S., et al. (2012). Physicochemical characterization of hemicelluloses from bamboo (*Phyllostachys pubescens* Mazel) stem. *Industrial Crops and Products*, *37*(1), 41–50.

Peng, H., Zhang, J. S., Liu, Y. H., Liu, D. T., Yu, Z. P., Wan, Y. Q., et al. (2012). Structural characterization of hemicellulosic polysaccharides isolated from bamboo (*Phyllostachys pubescens* Mazel). *Current Organic Chemistry*, *16*(16), 1855–1862.

Peng, P., Peng, F., Bian, J., Xu, F., & Sun, R. C. (2011). Studies on the starch and hemicelluloses fractionated by graded ethanol precipitation from bamboo *Phyllostachys bambusoides* f. shouzhu Yi. *Journal of Agricultural and Food Chemistry*, *59*(6), 2680–2688.

Prozil, S. O., Costa, E. V., Evtuguin, D. V., Lopes, L. P. C., & Domingues, M. R. M. (2012). Structural characterization of polysaccharides isolated from grape stalks of *Vitis vinifera* L. *Carbohydrate Research*, *356*, 252–259.

Sandula, J., Kogan, G., Kacurakova, M., & Machova, E. (1999). Microbial (1→3)-β-D-glucans, their preparation, physico-chemical characterization and immunomodulatory activity. *Carbohydrate Polymers*, *38*(3), 247–253.

Skendi, A., Biliaderis, C. G., Izydorczyk, M. S., Zervou, M., & Zoumpoulakis, P. (2011). Structural variation and rheological properties of water-extractable arabinoxylans from six Greek wheat cultivars. *Food Chemistry*, *126*(2), 526–536.

Sun, N., Rahman, M., Qin, Y., Maxim, M. L., Rodríguez, H., & Rogers, R. D. (2009). Complete dissolution and partial delignification of wood in the ionic liquid 1-ethyl-3-methylimidazolium acetate. *Green Chemistry*, *11*(5), 646–655.

Sun, X. F., Jing, Z. X., Fowler, P., Wu, Y. G., & Rajaratnam, M. (2011). Structural characterization and isolation of lignin and hemicelluloses from barley straw. *Industrial Crops and Products*, *33*(3), 588–598.

Sun, X. F., Sun, R. C., Fowler, P., & Baird, M. S. (2005). Extraction and characterization of original lignin and hemicelluloses from wheat straw. *Journal of Agricultural and Food Chemistry*, *53*(4), 860–870.

Sun, Y. C., Wen, J. L., Xu, F., & Sun, R. C. (2011). Structural and thermal characterization of hemicelluloses isolated by organic solvents and alkaline solutions from *Tamarix austromongolica*. *Bioresource Technology*, *102*(10), 5947–5951.

Tian, Y. T., Zeng, H. L., Xu, Z. B., Zheng, B. D., Lin, Y. X., Gan, C. J., et al. (2012). Ultrasonic-assisted extraction and antioxidant activity of polysaccharides recovered from white button mushroom (*Agaricus bisporus*). *Carbohydrate Polymers*, *88*(2), 522–529.

Vazquez, G., Antorrena, G., Gonzalez, J., & Freire, S. (1997). FTIR, H-1 and C-13 NMR characterization of acetosolv-solubilized pine and eucalyptus lignins. *Holzforschung*, *51*(2), 158–166.

Wen, J. L., Xiao, L. P., Sun, Y. C., Sun, S. N., Xu, F., Sun, R. C., et al. (2011). Comparative study of alkali-soluble hemicelluloses isolated from bamboo (*Bambusa rigida*). *Carbohydrate Research*, *346*(1), 111–120.

Wilkie, K. C. B., & Woo, S. L. (1976). Non-cellulosic β-D-glucans from bamboo, and interpretative problems in the study of all hemicelluloses. *Carbohydrate Research*, *49*, 399–409.

Wilkie, K. C. B., & Woo, S. L. (1977). A heteroxylan and hemicellulosic materials from bamboo leaves, and a reconsideration of general nature of commonly occurring xylans and other hemicelluloses. *Carbohydrate Research*, *57*, 145–162.

Xiao, B., Sun, X. F., & Sun, R. C. (2001). Chemical, structural, and thermal characterizations of alkali-soluble lignins and hemicelluloses, and cellulose from maize stems, rye straw, and rice straw. *Polymer Degradation and Stability*, *74*(2), 307–319.

Xie, J., Lin, Y. S., Shi, X. J., Zhu, X. Y., Su, W. K., & Wang, P. (2013). Mechanochemical-assisted extraction of flavonoids from bamboo (*Phyllostachys edulis*) leaves. *Industrial Crops and Products*, *43*, 276–282.

Yang, D., Zhong, L. X., Yuan, T. Q., Peng, X. W., & Sun, R. C. (2013). Studies on the structural characterization of lignin, hemicelluloses and cellulose fractionated by ionic liquid followed by alkaline extraction from bamboo. *Industrial Crops and Products*, *43*, 141–149.

Yang, H. P., Yan, R., Chen, H. P., Hee, D. H., & Zheng, C. G. (2007). Characteristics of hemicellulose, cellulose and lignin pyrolysis. *Fuel*, *86*(12–13), 1781–1788.

Yang, H. P., Yan, R., Chen, H. P., Zheng, C. G., Lee, D. H., & Liang, D. T. (2006). In-depth investigation of biomass pyrolysis based on three major components: Hemicellulose, cellulose and lignin. *Energy and Fuel*, *20*(1), 388–393.

Ying, Z., Han, X. X., & Li, J. R. (2011). Ultrasound-assisted extraction of polysaccharides from mulberry leaves. *Food Chemistry*, *127*(3), 1273–1279.

Yuan, T. Q., Sun, S. N., Xu, F., & Sun, R. C. (2011). Characterization of lignin structures and lignin–carbohydrate complex (LCC) linkages by quantitative 13C and 2D HSQC NMR spectroscopy. *Journal of Agricultural and Food Chemistry*, *59*(19), 10604–10614.

Zeng, W. C., Zhang, Z., Gao, H., Jia, L. R., & Chen, W. Y. (2012). Characterization of antioxidant polysaccharides from *Auricularia auricular* using microwave-assisted extraction. *Carbohydrate Polymers*, *89*(2), 694–700.

Zhang, Y., Jiao, J. J., Liu, C. M., Wu, X. Q., & Zhang, Y. (2008). Isolation and purification of four flavone C-glycosides from antioxidant of bamboo leaves by macroporous resin column chromatography and preparative high-performance liquid chromatography. *Food Chemistry*, *107*(3), 1326–1336.